

Auto-VTNA: An Automatic VTNA platform for Determination of Global Rate Equations

Daniel Dalland, Linden Schrecker* and King Kuok (Mimi) Hii

Department of Chemistry, Imperial College London, Molecular Sciences Research Hub, 82, Wood Lane, London W12 0BZ, U.K.

Abstract

The ability and desire to generate kinetic data has greatly increased in recent years, requiring more automated and quantitative methods for analysis. In this work, an automated program (Auto-VTNA) is developed, to simplify the kinetic analysis workflow. The Auto-VTNA solver allows all the reaction orders to be determined concurrently, expediting the process of kinetic analysis. Auto-VTNA performs well on noisy or sparse data sets and can handle complex reactions involving changing reaction orders. Quantitative error analysis and facile visualisation allows users to numerically justify and robustly present their findings. Auto-VTNA can be used through a free graphical user interface (GUI), requiring no coding or kinetic knowledge from the user, or can be customised and built on if required.

Introduction

The study of chemical kinetics supports our mechanistic understanding of chemical reactions and is crucial for the development of safe and efficient synthetic procedures on scale.^{1,2,3,4} Chemical kinetics is also utilized extensively to understand and optimize the behaviour of reaction systems, particularly complex catalytic reactions.⁵⁻⁹ The global rate equation (a.k.a. the rate law) is a mathematical expression that correlates the rate of a reaction with the concentration of each reaction species, with the general form:

$$rate = k[A]^m[B]^n[C]^p \quad (Eq. 1)$$

Where [A], [B] and [C] = the molar concentrations of the reacting components (reactants, catalyst, products); k = rate constant; and m , n and p = the orders of the reaction with respect to each reaction component.

A global rate equation can be constructed empirically from experimental data, without explicit considerations of the reaction mechanism or mass transfer effects.^{10,11} Traditionally, kinetic experiments include “flooding”^{12,13} or the initial rates method.^{14,15} While these methods are generally easy to analyse (as the data can be linearized), the results must be treated with caution, as they are either performed under non-synthetically relevant conditions,^{4 14,15} or cannot detect changes in

reaction orders associated with more complex mechanisms, such as catalyst deactivation or product inhibition.¹⁶

In the past few decades, modern advances in process analytical tools and computing power have greatly accelerated the development of data-rich kinetic experiments under synthetically relevant conditions. In the late 1990's, Blackmond pioneered the development of Reaction Progress Kinetic Analysis (RPKA),^{17–19} which greatly streamlines the determination of rate laws from a series of “same excess” and “different excess” experiments.^{4,5} The experimental data can be manipulated in an electronic spreadsheet to obtain overlays between rate vs concentration plots to obtain individual reactant order. Later, this was expanded to “time adjusted” concentration vs time plot,⁶ which was further elaborated by Burés in 2016, into Time Normalization Analysis (TNA) for determining catalyst order; later in the same year, this was further extended to all reacting species, called “Variable Time Normalization Analysis” (VTNA),¹⁸ based on numerical integration of the rate equation. One of the most attractive features of these visual kinetic analysis tools is that reaction orders can be derived by visual inspection of reaction profile overlay, without the need for complex mathematical calculations or bespoke software, hence making them more accessible to the synthetic chemistry community.^{8,20–22}

In the last few years, the widespread popularity of Python as a general programming language has greatly accelerated the automation of machine-readable tasks. Recently, Hein and co-workers have developed a Python package “Kinalite”, a simple API for performing VTNA.²³ Kinalite requires kinetic data from each experiment to be imported as individual csv files, containing time-concentration data of different reaction species. The user selects a reaction species and two relevant experimental data to determine the reaction order automatically. For multiple species, or for more than two data series, this process must be performed sequentially, determining one species order at a time. The package presents the result as a plot of ‘errors’ associated with different order values for a specific reaction species, demonstrating the best order value.^{24,25} These individually calculated orders can be combined to yield the global rate equation. By removing the need for visual inspection, Kinalite removes human bias. However, there are remaining issues:

1. Only data from two experiments can be analysed at a given time.
2. Only the order of one reaction species can be determined at a given time.

3. Kinalite's method for assessing concentration profile overlay causes it to generate rugged "error plots" and fails when concentration profiles with sufficiently different time domains are compared.

In this work, we will describe the development of a new and more robust Python package to perform VTNA that can execute multiple fittings of reaction orders *simultaneously*. Apart from significant time saving, an unlimited number of initial concentrations can be altered between experiments by computationally assessing the overlay across a wide range of order value combinations. This presents a novel way of carrying out "different excess" experiments which avoids the systematic errors of stock solutions and improves the amount of kinetic information obtained per run.

Method

The auto-VTNA programme offers the following features:

1. Manual and automatic VTNA in a more time efficient manner;
2. VTNA with several normalised reaction species;
3. Visualisation of overlay score across different reaction orders;
4. Quantification of error analysis;
5. Improved accessibility.

Each of these features will be presented below as a 'unique selling point' (USP) of the package, followed by a result and discussion, where the application of the auto-VTNA is showcased with several examples.

USP1: Automatic VTNA in Python.

Traditionally, VTNA involves normalising the time axis of concentration time data with respect to a particular reaction species, whose initial concentration varies across different experiments. Several reaction orders are entered in a spreadsheet by trial-and-error, until the order giving the best visual overlay of the concentration profiles is identified. Concentration profiles linearise if the time axis is normalised with respect to every reaction component raised to its correct order.^{8,26,27} However, most examples of VTNA involve overlay of non-linear monotonically increasing or decreasing product or reactant concentration profiles (Fig. 1).^{7,20,31}

To develop a robust automated method, we began by emulating the manual routine within a Python script that calculates the transformed time axis for a chosen reaction species and corresponding order value(s) using a selected subset of the kinetic data, tested on literature examples (see section S8).²⁸ Subsequently, a robust automatic method of assessing the overlay of reaction progress profiles

was developed removing the need for manual visual inspection. This method involves fitting all profiles to a common flexible function and utilizing a goodness-of-fit score (e.g. RMSE), as an ‘overlay score’, to quantify the degree of overlay.

In order to process non-linear fitting, a 5th order monotonic polynomial fitting, a statistical method with several scientific applications,^{29,30} was selected as the default method. Although a more efficient ordinary polynomial fitting can be selected that is 10 times faster, there is an increased risk of overfitting effects on the overlay score, especially for reaction profiles with few datapoints. Additionally, Auto-VTNA allows linear fitting, which is particularly useful when reaction profiles linearise upon complete normalisation of the time axis (Section S3, Supporting Info).

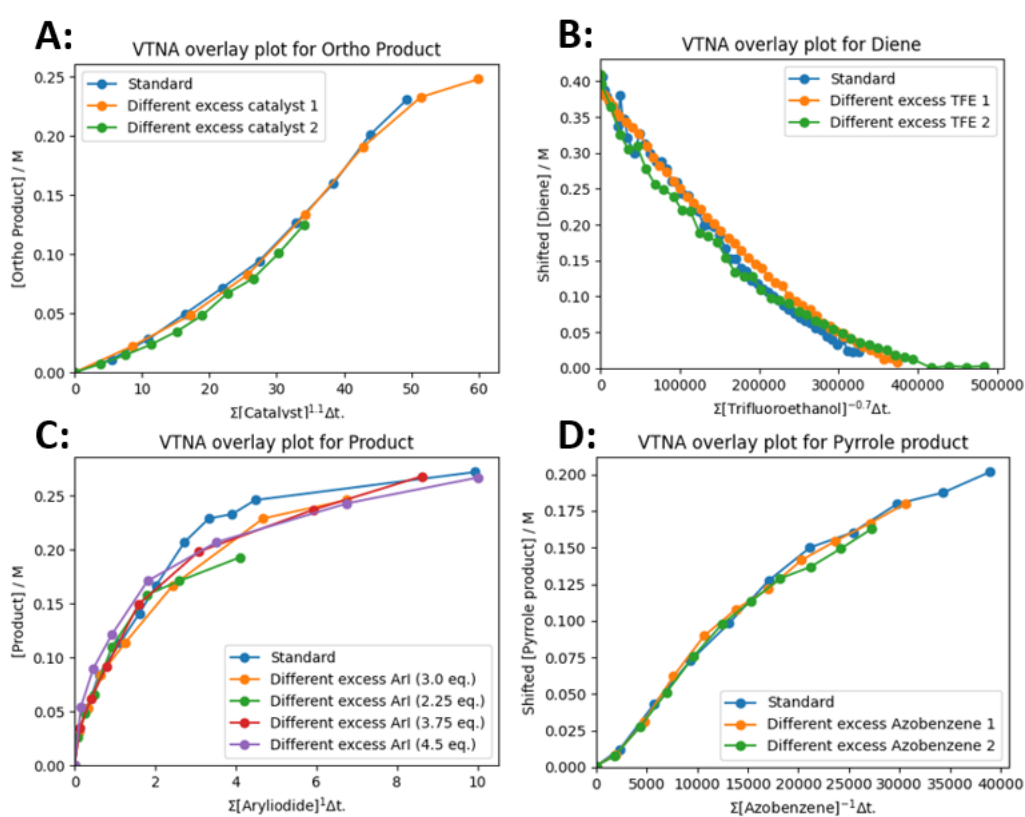


Figure 1. VTNA overlay plots from literature with the reported order values giving concentration profile overlay.^{31–34}

The method of assessing the goodness-of-fit *via* an ‘overlay score’ is different from that employed in Kinalite, which relies on the difference in y-axis values of datapoints when sorted by transformed time value (‘error’) (see section S2.2). This ‘error’ measure in some cases yields results that are inaccurate compared to the best overlay by visual inspection, especially if the density of the two compared data series are different, reducing the level of automation provided by Kinalite.²⁵ In contrast, Auto-

VTNA has reliably yielded the order value(s) that maximise concentration profile overlay as judged by visual inspection on all tested examples.

Upon establishing a robust method for computationally assessing the degree of concentration profile overlay, an algorithm was developed to perform automatic VTNA and embedded into a Python package, which we named “Auto-VTNA”.

USP2: VTNA with several normalised reaction species

Unlike previous methods, Auto-VTNA can be used to identify the order values for several reaction species in the same calculation, generating a better understanding of how a change in one order value may affect another. The basic workflow is demonstrated in Figure 2. Firstly, a mesh with a selected number of order values within a specified range is defined, e.g. from -1.5 to 2.5 (step 1). Secondly, a list of every combination of reaction order values for each normalised species is created (step 2). For each combination of orders, the time axis is normalised, and the transformed concentration profiles fitted to obtain the overlay score (step 3 and 4). This reveals the optimal order combination around which a new collection of order value combinations is generated to increase the precision with which the optimal reaction orders are determined (steps 5 and 6). This procedure is repeated a selected number of times to increase precision without an unacceptably high processing time (Fig. S3).

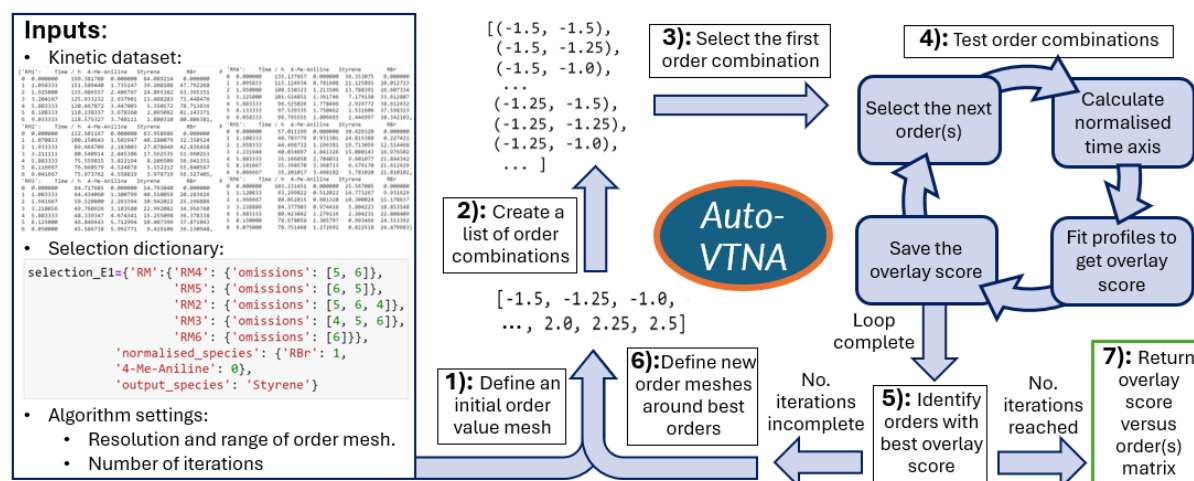


Figure 2. Flowchart illustrating the basic workflow of the Auto-VTNA algorithm.

Traditional “different excess” experiments only alter the initial concentration of one reaction species at a time to facilitate traditional VTNA. Auto-VTNA can determine the reaction orders of several reaction species simultaneously. This facilitates more efficient “different excess” experiments, where the initial concentration of several reaction species is altered between experiments. Thus, the number

of experiments required to determine reaction orders for multi-component reaction systems can be reduced.

USP3: Visualising the results of automatic VTNA

Conventionally, VTNA results are presented by comparing “bad” with “optimal” overlays (Fig. 3a). In contrast, Auto-VTNA offers a more detailed visualisation of how changing order values affects overlay (Fig. 3b). As the degree of reaction profile overlay is calculated for a range of different order values, a plot of overlay score against order value(s) can be produced. Thus, researchers utilising this method can justify the optimal reaction order in a quantifiable manner.

Through its “error” metric, Kinalite can also produce a rudimentary overlay score (Fig. 3c), which produces almost the same order assignment as Auto-VTNA for the simulated kinetic data in figure 3a. However, its reduced reliability becomes evident from the erratic curve produced, particularly at negative order values.

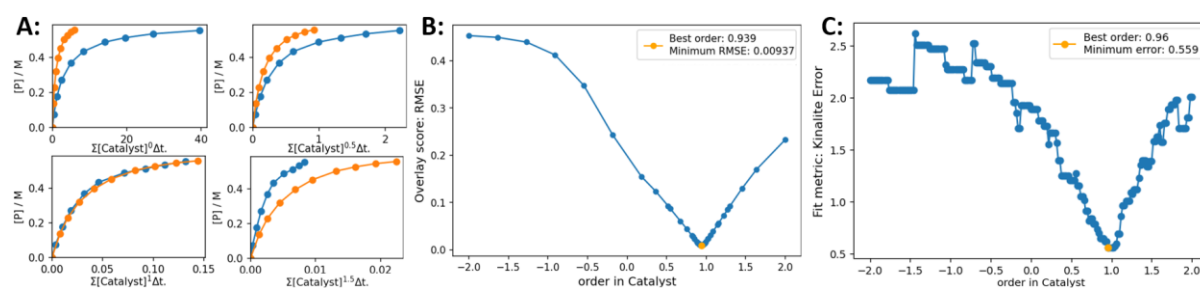


Figure 3. A: Overlay plots for simulated data involving the catalytic conversion of reactants $A + B \rightarrow P$, including catalyst decomposition.¹⁹ B: Plot showing the overlay scores (RMSE of 5th order monotonic polynomial fits) against the reaction order in catalyst. C: Corresponding “error plot” obtained using Kinalite.

When Auto-VTNA is solving the reaction orders of two reacting species, the correlation between the overlay score and the combinations of order values can be visualised by a contour plot (Fig. 4). If the algorithm is set to obtain the reaction orders of three or more reaction species, overlay scores can be tabulated for a selected number of order value combinations. However, in this case, the results are challenging to visualise due to the higher dimensionality of the data. Alternatively, if a reaction order in a species is already known, this can be inputted as a fixed value and the algorithm calculates the overlay score as a function of the remaining species. This lowers the dimensionality of the order versus overlay score matrix so that the results can be visualised by a graph or contour plot.

The graphs and contour plots generated by Auto-VTNA (Fig. 3 and 4, respectively), allow individual overlay plots to be produced in an interactive manner through mouseclicks (Fig. 4). By left-clicking on the graph or contour plot, a traditional overlay plot is generated, whereas right-clicks show the plot

with normalised y axis, the fitted function and the overlay score of the click order value(s). This allows the operator to interrogate the overlay score landscape obtained by Auto-VTNA and verify that the optimal reaction order(s) give optimal concentration profile overlay.

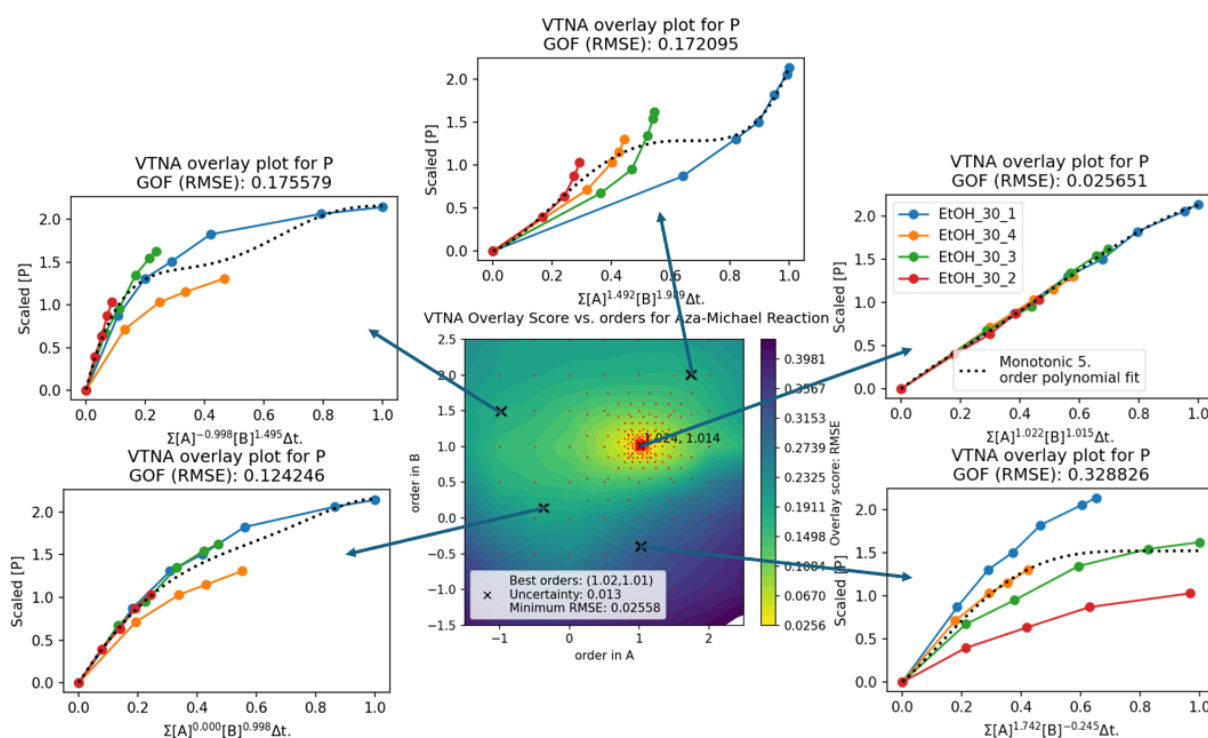


Figure 4. VTNA overlay plots generated using kinetic data on the Aza-Michael reaction between piperidine (**2**) and methyl itaconate (**1**).³⁵ The overlay plots are generated by right-clicking the contour plot.

USP4: Error analysis

Certainty in a set of order values can also be assessed through automatic calculation of the range in which the overlay score for a set of order values is no greater than 15% (by default) from the optimal overlay score. For example, the assigned order of 0.954 shown in Figure 5 has a 15% overlay score interval of (0.912, 0.987) whereas the interval for Figure 3 is (1.001, 1.008) and (1.008, 1.022) for the respective reactants, reflecting a more well-defined overlay score minimum point, as expected for simulated data. The range of order value combinations within this cut-off can be visualised as blue dots in the contour plot (Fig. 5A) or represented by an orange line if the order in only one species is investigated (Fig. 5B).

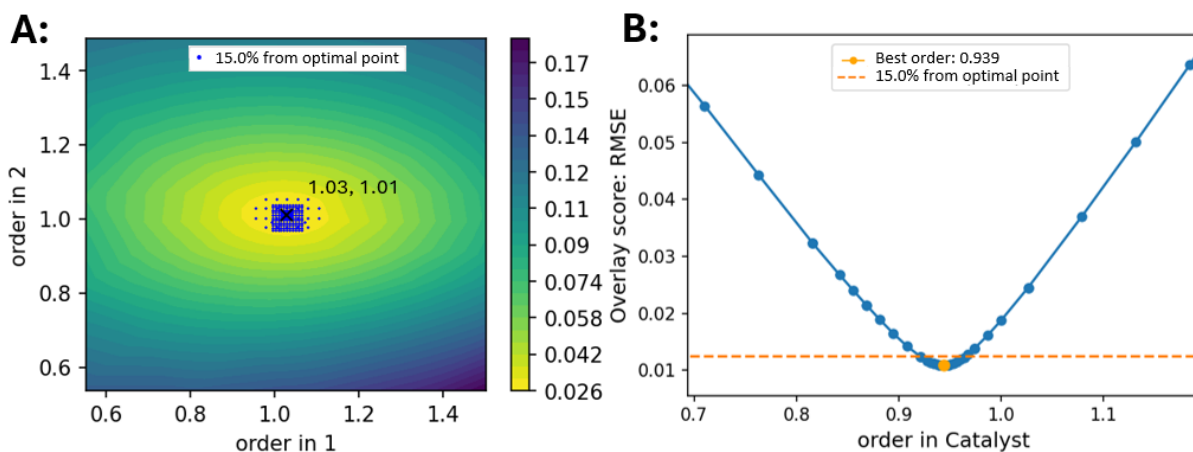


Figure 5. A: Contour plot illustrating the degree of concentration profile overlay across different reaction order values in **1** and **2** for data on their aza-Michael addition in EtOH (*vide infra*).³⁶ The blue dots illustrate the order combination values with overlay scores within 15% of the optimal point at (1.03,1.02). B: Overlay score vs. order in catalyst for simulated kinetic data.¹⁹

The interpretation of this overlay score can provide valuable information of the reaction under study. The *absolute* optimal overlay score reflects effects that can lower the confidence in the global reaction order afforded by VTNA, such as noisy kinetic data, insufficient data point density for accurate numerical integration, as well as more complex reaction mechanisms giving changing order values, e.g. catalyst deactivation. To improve the utility of absolute overlay score values, it is necessary to limit the influence of factors other than the degree of concentration profile overlay. For example, to prevent the concentration scale from influencing goodness-of-fit values, Auto-VTNA scales and normalises the y-axis prior to generating the overlay score by fitting all reaction profiles to the same polynomial. Moreover, the effect of over- and under-fitting on the overlay score is limited by employing a flexible 5th order monotonic polynomial fit (Section S3, Supporting info). Lastly, to facilitate the comparison of overlay scores obtained with different datasets, RMSE has been set as the default goodness-of-fit measure (Section S4, Supporting info).

USP5: Improved accessibility

Last but not least, an open-source graphical user interface (GUI) named “Auto-VTNA Calculator” was developed. This provides access to the benefits of Auto-VTNA without requiring knowledge of Python coding. Upon uploading kinetic data as an Excel or multiple csv files, dropdown menus allow the experiments, reaction species for time axis normalisation, and the output species to be selected for VTNA or Auto-VTNA analysis. Calculation and data visualisation features can be adjusted in settings menus, and the results from automatic VTNA can be saved as an Excel or csv file. A “Crop Data” feature can be used to streamline the modification of the input data to investigate the impact on reaction

order values, for example, to remove outliers, or to truncate excess data points recorded after reaction completion (Fig. 6).

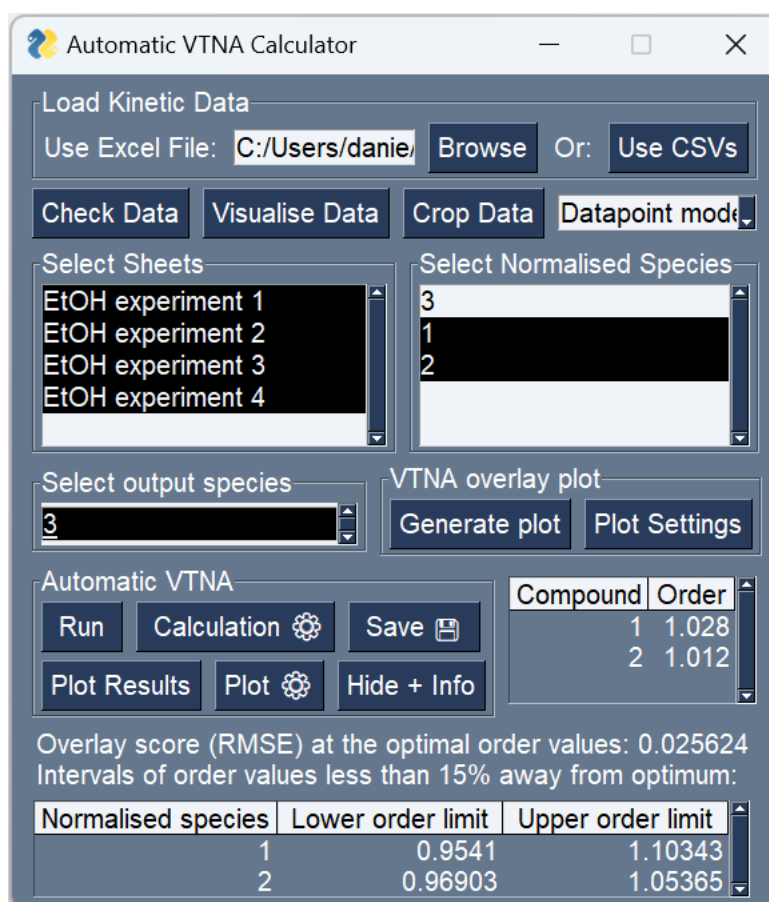
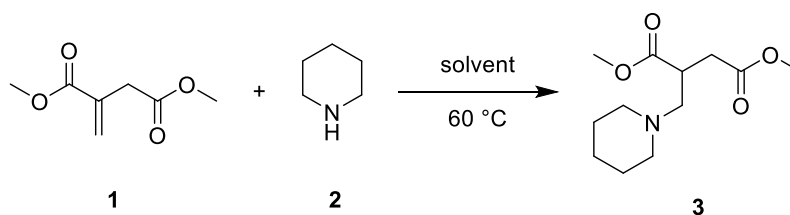


Figure 6. The graphical user interface of the Auto-VTNA dashboard.

Results and discussion

The reliability and functionality of Auto-VTNA were evaluated by the analysis of kinetic data previously reported in literature and comparing the results. The first chosen example was the aza-Michael addition of piperidine **2** to dimethyl itaconate **1** (Scheme 1)³⁷ reported by Clark *et al.*³⁵ Interestingly, the reaction order were reported to change in different solvents: Previous VTNA suggested that the reaction order in the piperidine was 1 in ethanol, 2 in DMSO and THF, but 1.6 in IPA.



Scheme 1. Aza-Micheal addition of piperidine **2** to dimethyl itaconate **1**.³⁵

Utilising the Auto-VTNA Calculator with default settings (5th order monotonic fitting with an RMSE overlay score), reaction orders in **1** and **2** were identified for the ethanol, IPA, THF, and DMSO datasets (Table 1) within 3 minutes. Generally, the Auto-VTNA derived order values match the orders reported within 0.1 and gave equal or better concentration profile overlay than that obtained using reported orders (Fig. S5, Supporting Info). An exception is the reaction in DMSO, for which the computed reaction orders of 0.77 and 1.86 deviated more significantly from the reported order values of 1 and 2. This is attributed to the sparsity of kinetic data obtained from the reaction DMSO (3 experiments with 4 time points each), which leads to a greater influence of random errors and inaccurate numerical integration. The results from each calculation can be represented as contour plots (Fig. 7), showing well-defined overlay score minima around the best order values, in particular for the ethanol dataset.

Table 1. Comparison of reported and reanalysed reaction orders for the *aza*-Michael reaction of dimethyl itaconate **1** and piperidine **2**.

Solvent	Reported value	Auto-VTNA
EtOH	$[1]^1[2]^1$	$[1]^{1.03}[2]^{1.01}$
IPA	$[1]^1[2]^{1.6}$	$[1]^{1.00}[2]^{1.66}$
DMSO	$[1]^1[2]^2$	$[1]^{0.77}[2]^{1.93}$
THF	$[1]^1[2]^2$	$[1]^{0.94}[2]^{1.86}$

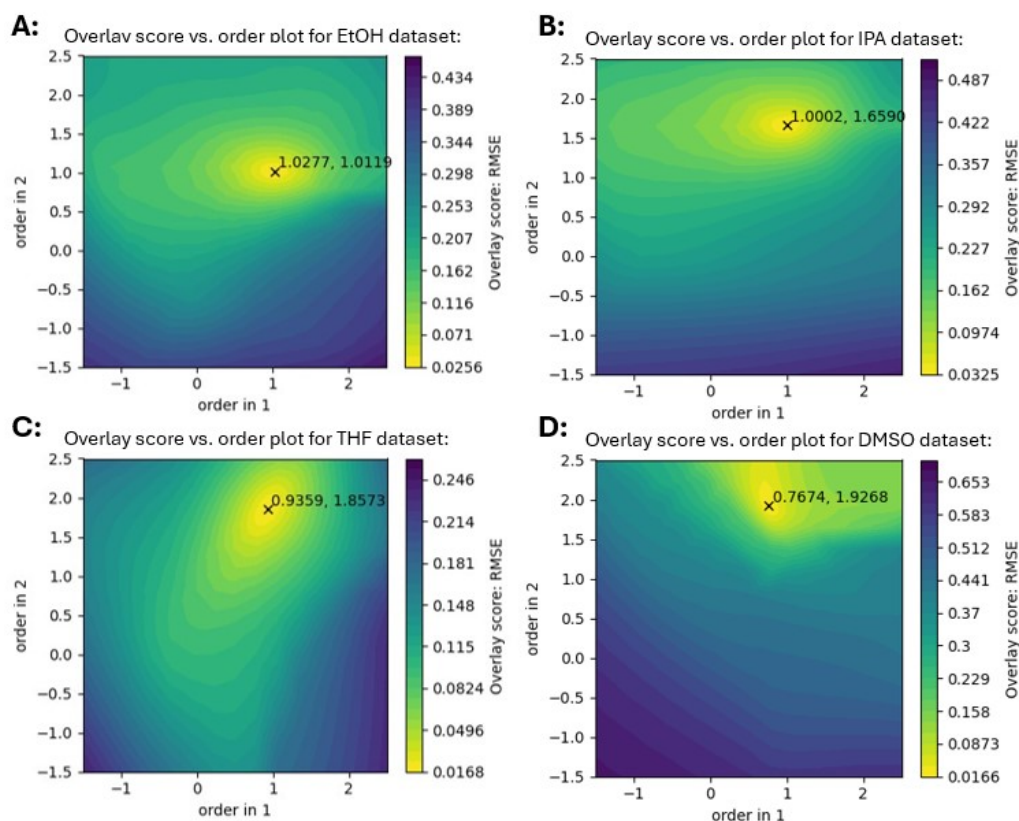


Figure 7. Contour plots illustrating the degree of concentration profile overlay as the RMSE of the total fit against the reaction order in dimethyl itaconate 1 and piperidine 2 in EtOH (A), IPA (B), THF (C) and DMSO (D).

Overall, this example illustrates that Auto-VTNA reliably computes order values based on optimal concentration profile overlay that match reported orders obtained by visual inspection. Moreover, computationally derived order values which deviate from the expected integer values could motivate researchers to improve the kinetic data quantity and quality.

Automatic determination of rate equations using Auto-VTNA

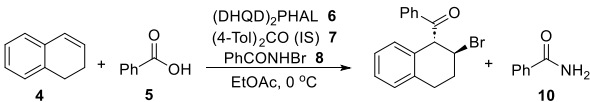
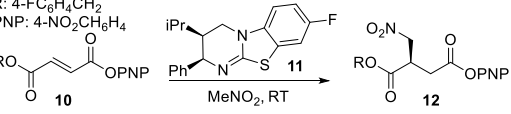
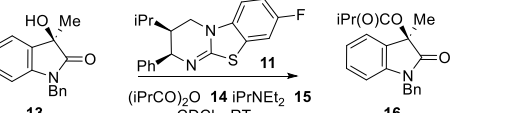
Following from this, auto-VTNA was applied to kinetic data from 22 publications, including stoichiometric and catalytic reactions (Table 4, entries 1-14) containing up to 6 reaction species (reactants, reagents, catalyst and additives).^{5,8,9,34,37-46} The current approach to VTNA experimentation involves performing a “standard” reaction, under synthetically relevant conditions, followed by “different excess” experiments, where only the initial concentration of each reaction species is altered. This experiment design we define as “sequential VTNA”, as the orders are obtained for one reaction species at a time by identifying the order that makes the standard and relevant different excess profiles overlay. Pleasingly, we found that Auto-VTNA with a 5th order monotonic fit function could identify the order values giving optimal overlay at every attempt using sequential VTNA. However, for one dataset

with trimolecular kinetic data involving overlay of step-like reaction profiles, a 9th order polynomial was required to avoid underfitting (Section S3, Supporting Info).

In “total-VTNA”, all experiments are combined and normalised with respect to every reaction species for which an order has been obtained via sequential VTNA. If every reaction species contributing to the rate has been normalised, linearisation occurs so that the observed rate constant can be derived.^{7,8,37,40–42,46,47} However, barring some possible exceptions^{41,44}, total VTNA is not currently used to derive reaction orders. Auto-VTNA enables the determination of the reaction orders of an unlimited number of reaction species in one single calculation, bypassing the sequential VTNA approach. This enables researchers to vary more than one initial concentration at the time, increasing the information content per reaction run, and lowering the signal to noise ratio for the total VTNA calculation. This change from sequential to total VTNA is analogous to the improvement offered by design of experiments over the one-factor-at-the-time (OFAT) for reaction optimisation.

Currently, there are few reported kinetic studies in which more than one initial concentration was varied between each different excess experiments.^{35,44} Nonetheless, as long as the concentration profiles of every reaction species has been measured or can be inferred from the product profiles, total VTNA can also be applied to ordinary VTNA datasets. This was performed for kinetic data obtained from 15 publications.^{5,8,9,34,37–45,47–50} Two of these publications were omitted as sequential VTNA had revealed that reaction orders change with the initial concentrations of reactants.^{38,50} Kinetic data from the remaining 13 publications was re-analysed by Auto-VTNA sequentially (Table SX) and by automatic total VTNA (Table 2).

Table 2. VTNA datasets for catalytic reaction systems from literature with reported and calculated reaction order values.

Entry	Reaction system	Reported orders	Calculated orders
1 ⁴³		$[4]^1 [5]^1$ $[6]^1 [8]^1$	$[4]^{1.00} [5]^{1.04}$ $[6]^{1.02} [8]^{1.01}$
2 ³⁷		$[10]^1 [11]^1$ $[12]^{-0.5}$	$[10]^{0.94} [11]^{0.99}$ $[12]^{-0.49}$
3 ⁴²		$[13]^{0.9} [11]^{1.0}$ $[14]^{1.0} [15]^0$	$[13]^{0.95} [11]^{1.02}$ $[14]^{1.06} [15]^{0.04}$

4 ⁴⁶		[17] ¹ [18] ¹ [19] ¹	[17] ^{1.00} [18] ^{0.95} [19] ^{0.91}
5 ⁴⁵		[21] ^{0.85} [22] ^{-0.6} [23] ^{0.9}	[21] ^{0.90} [22] ^{-0.58} [23] ^{0.94}
6 ⁴⁴		[25] ¹ [26] ¹ [27] ¹	[25] ^{0.92} [26] ^{0.97} [27] ^{0.96}
7 ⁴⁷		[29] ^{1.5} [30] ¹ [31] ^{0.15}	[29] ^{1.51} [30] ^{1.18} [31] ^{0.20}
8 ⁵		[32] ⁻¹ [33] ¹ [34] ¹	[32] ^{-1.07} [33] ^{1.05} [34] ^{1.12}
9 ⁵		[32] ⁻¹ [33] ¹ [34] ¹	[32] ^{-0.44} [33] ^{0.99} [34] ^{1.19}
10 ⁸		[36] ¹ [37] ^{0.75} [38] ¹ [39] ^{0.5} [40] ⁰ [41] ¹	[36] ^{1.07} [37] ^{0.60} [38] ^{1.02} [39] ^{0.30} [40] ^{-0.04} [41] ^{0.99}
11 ⁴⁴		[43] ⁰ [44] ^{0.9} [45] ^{1.1} [46] ¹	[43] ^{-0.03} [44] ^{0.62} [45] ^{1.26} [46] ^{0.86}
12 ⁴⁰		[48] ¹ [49] ⁰ [50] ⁰ [51] ¹	[48] ^{0.86} [49] ^{0.13} [50] ^{-0.07} [51] ^{0.95}
13 ⁴¹		[53] ^{2.05} [54] ^{0.78} [55] ^{-0.03} [56] ^{0.20} [22] ^{0.02}	[53] ^{0.97} [54] ^{0.60} [55] ^{0.11} [56] ^{0.18} [22] ^{0.10}
14 ³⁴		[59] ⁰ [60] ¹ [61] ¹	[59] ^{0.191} [60] ^{1.31} [61] ^{1.05}

For entries 1-8 of Table 2, Auto-VTNA for both sequential and total VTNA yielded order values in close agreement with the reported values. The 15% uncertainty intervals for the optimal order values were also moderate for these datasets. For entries 9-12 of table 2, the order values obtained by automatic total VTNA deviate more significantly from the reported values. However, as demonstrated in section SX, the calculated order values demonstrate closer overlay than the reported values. Entry 13 of table 2 yielded order values in close agreement with those reported, with the exception of the order in the alkyne which was found to be 1.05 rather than 2.05 (Figure SX). Entry 14 of table 2 is based on kinetic

data with high uncertainty intervals both in sequential and total VTNA, suggesting that more experiments should be conducted to confirm the rate equation.

The reaction orders determined by Auto-VTNA yielded superior overlay scores compared to those presented in the original publication (see section SX). For example, kinetic data on the cyclopropanation of styrene with dirhodium tetracarboxylate catalysts recorded by Wei *et al.*⁵ was re-analysed to obtain orders consistent with the reported values, although with a catalyst order of 1.12 rather than 1.0 which is consistent with catalyst inhibition (Figure 8 and table 2, entry 8).⁵ The same excess run was included in the calculation to further improve reaction order accuracy, illustrating the power of varying more than one initial concentration per run.

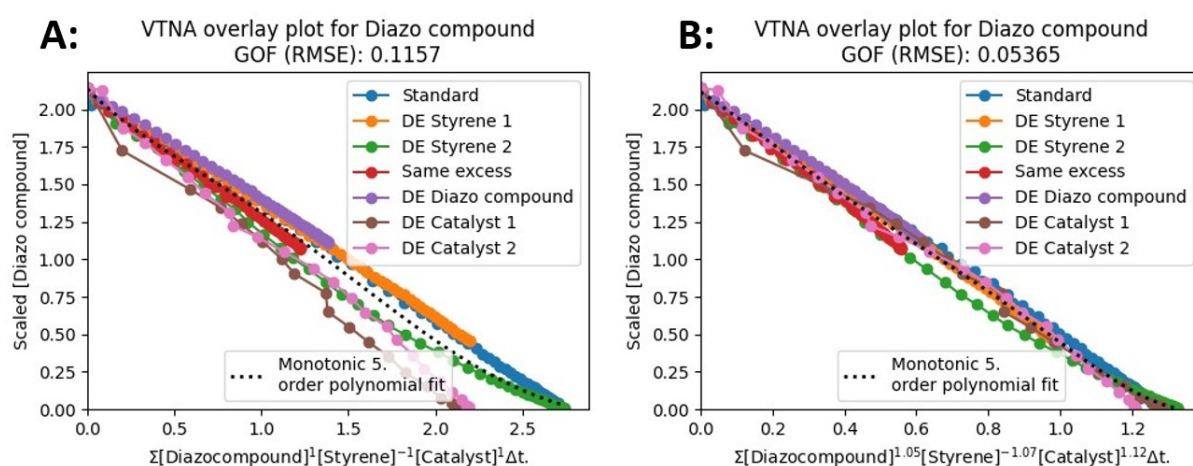


Figure 8. VTNA overlay plots illustrating the degree of concentration profile overlay achieved by total VTNA using: (A) the reported order values; (B) and those calculated using Auto-VTNA.⁵

We also applied Auto-VTNA to the analogous kinetic dataset recorded by Wei *et al.* in dimethylcarbonate (table 2, entry 9) which was found to be less consistent. We hypothesised that by including all experiments indiscriminately, the noise caused by poorly controlled factors such as water concentration would cancel out to reveal the true orders. While the calculated order in diazo compound matched the reported value of 1, the order in styrene was lower than initially reported, suggesting that styrene inhibition is less severe in dimethylcarbonate. The order in catalyst was again found to be greater than the reported value of 1.

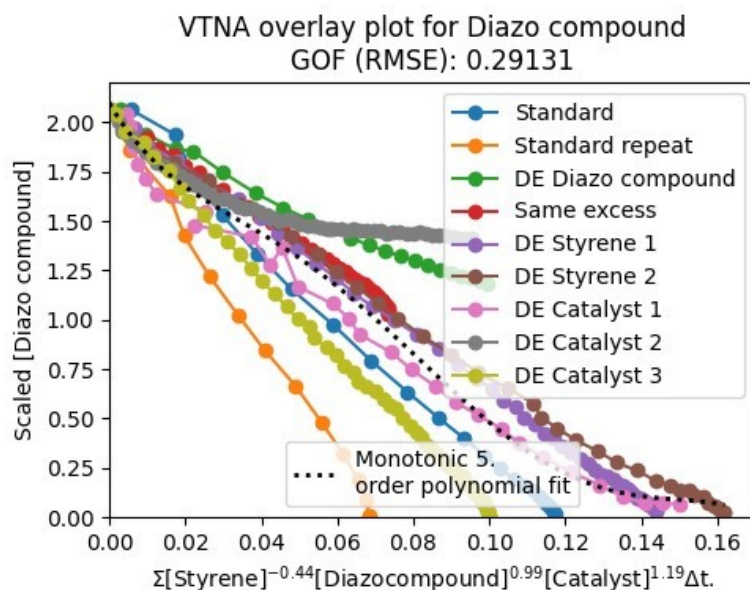


Figure 9. VTNA overlay plot with the reaction order values obtained using Auto-VTNA for the diazo compound mediated cyclopropanation of styrene in the presence of a dirhodium tetracarboxylate catalyst.

The kinetic study of Lancaster *et al.* on a catalytic asymmetric alkene bromoesterification reaction (table 2, entry 1) represents a good example on the power of automatic total VTNA for elucidating rate equations for catalytic reaction systems (Fig 10A). Using Auto-VTNA the analysis could be expanded to include same excess and product doping experiments, revealing an order of -0.75 in the amide by-product and an order of 0 in the desired product (Fig. 10B). The linearisation achieved by also normalising the time axis with respect to the inhibitory by-product indicates that the complete rate equation has been elucidated, allowing the observed rate constant to also be determined.

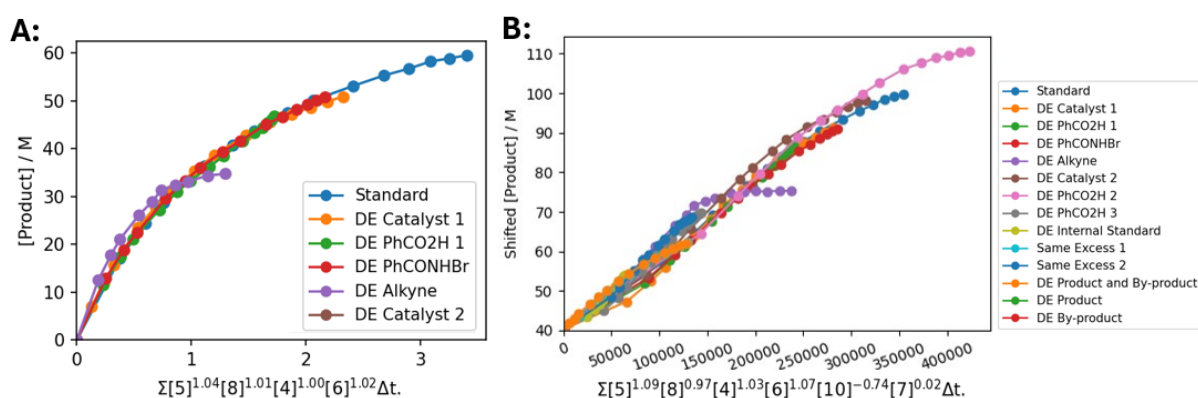


Figure 10. VTNA overlay plots obtained utilising Auto-VTNA for the catalytic asymmetric alkene bromoesterification reaction reported by Lancaster *et al.* analysed for: (A) all reactants and catalyst; and (B) all species present in the reaction including product, by-product, and internal standard.

Heck reaction with low Pd loading

In the final example, auto-VTNA was applied to analyse product concentration profiles for kinetic data by Newton *et al.* for the Heck reaction between iodobenzene and methyl acrylate catalysed by varying amounts of $\text{Pd}(\text{OAc})_2$,⁹ where it was reported that the catalyst order is dependent on catalyst loading, due to the presence of more than one active catalyst species, and different catalyst deactivation rates. Investigation utilising Auto-VTNA emulated the reported results: for low catalyst loading experiments (30, 50, 100 and 200 ppm), a catalyst order of 1.73 was identified, close to the reported value of 1.7; while a lower catalyst order of 0.87 was obtained for higher catalyst loadings (200, 400, 600, 800 and 1000), similar to the reported value of 0.9. The concentration profiles with high catalyst loadings exhibited a wider interval of reaction order values with overlay scores only 15% above the minimum (0.79 to 0.94 versus 1.70 to 1.77) as well as a higher overlay score at the optimal catalyst order (0.041 versus 0.023) (Fig. 11).

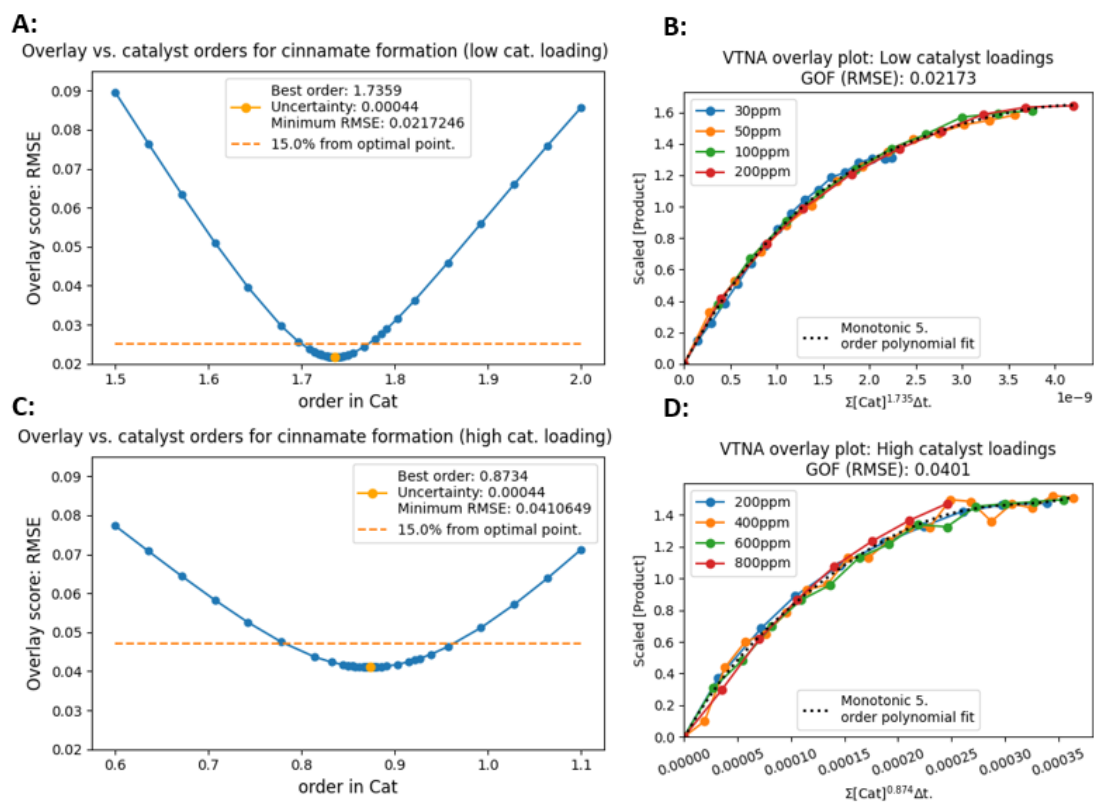


Figure 11. Graphs illustrating overlay score versus order in catalyst for low (A) and high (C) catalyst loadings (the y-axis ranges and the size of the x-axis domain are identical to facilitate comparison) and VTNA overlay plots at the best order values for low (B) and high (D) catalyst loadings respectively along with the fitted monotonic 5th order polynomial.

To investigate whether the reported catalyst order step change at 200 ppm is supported by Auto-VTNA, order values were calculated for pairs of experiments with consecutive catalyst loadings (Fig. 12).

Indeed, a step change is observed at 200 ppm in catalyst order value, although the catalyst order obtained from the 600 and 800 ppm experiments appears to be an outlier. The equivalent plots for order values obtained from groups of 3 or 4 experiments with consecutive catalyst loadings also indicate a step change from high to low catalyst orders, although less pronounced as the mid-range order values are obtained from concentration profiles from both the high and low catalyst loading domains (Fig. SAA12 and SAA13). This demonstrates the power of Auto-VTNA to quickly and accurately to provide kinetic analysis with robust quantified justification.

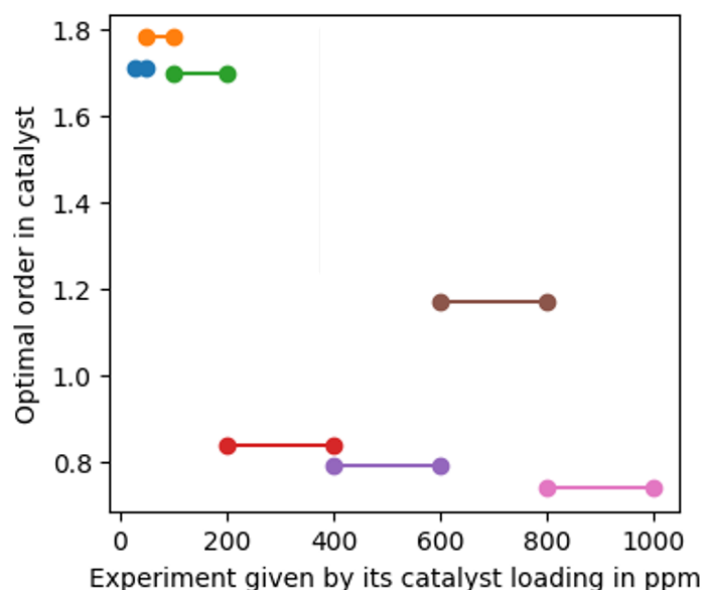


Figure 12. Calculated reaction orders in catalyst for consecutive pairs of product concentration profiles.

Conclusion

In summary, a robust method has been developed to automate VTNA. This mode of analysis simplifies data handling and enables automatic identification of the reaction order values giving concentration profile overlay for “different excess” experiments. Auto-VTNA utilizes a robust method for computationally assessing the degree of concentration profile overlay using a monotonic polynomial fitting procedure. To minimize processing time, the algorithm iteratively tests reaction order combinations, honing in on the optimal reaction order values. The results from Auto-VTNA can then be visualised as a graph or contour plot for 1 and 2 normalised reaction species respectively, a more efficient way to justify the reported reaction order values. Furthermore, Auto-VTNA can improve the assessment of uncertainty in assigned order values via overlay score intervals. Given that overlay score has been optimised to only reflect the degree of concentration profile overlay, the absolute overlay score also represents the uncertainty of the assigned orders.

Auto-VTNA was subsequently tested on kinetic data obtained from literature to demonstrate the key features and advantages.^{8,36} The ability to compute several reaction orders, utilising kinetic data obtained from multiple experiments (total-VTNA) is especially highlighted. The application of the method in a Heck reaction that involves changes in the catalyst order at different catalyst loadings was also demonstrated.

Last but not least, a graphical user interface has been made freely available, as well as the underlying code, to facilitate the use of Auto-VTNA by researchers. The program has been optimised for efficiency of use and does not require coding experience. It includes several features, such as removal of selected datapoints, kinetic data visualisation and interactive representation of Auto-VTNA results. We hope that this work will encourage wider adoption of VTNA by researchers to justify their assigned reaction order values in a more informative and efficient manner.

References

- (1) Kossoy, A.; Akhmetshin, Y. Identification of Kinetic Models for the Assessment of Reaction Hazards. *Process Safety Progress* **2006**, *25* (4), 326–330. <https://doi.org/10.1002/prs>.
- (2) Wagschal, S.; Broggini, D.; Cao, T. D. C.; Schleiss, P.; Paun, K.; Steiner, J.; Merk, A. L.; Harsdorf, J.; Fiedler, W.; Schirling, S.; Hock, S.; Strittmatter, T.; Dijkmans, J.; Vervest, I.; Van Hoegaerden, T.; Egle, B.; Mower, M. P.; Liu, Z.; Cao, Z.; He, X.; Chen, L.; Qin, L.; Tan, H.; Yan, J.; Cunière, N. L.; Wei, C. S.; Vuyyuru, V.; Ayothiraman, R.; Rangaswamy, S.; Jaleel, M.; Vaidyanathan, R.; Eastgate, M. D.; Klep, R.; Benhaim, C.; Vogels, I.; Peeters, K.; Lemaire, S. Toward the Development of a Manufacturing Process for Milvexian: Scale-Up Synthesis of the Side Chain. *Organic Process Research and Development*. American Chemical Society April 21, 2023, pp 680–691. <https://doi.org/10.1021/acs.oprd.2c00399>.
- (3) Wang, K.; Han, L.; Mustakis, J.; Li, B.; Magano, J.; Damon, D. B.; Dion, A.; Maloney, M. T.; Post, R.; Li, R. Kinetic and Data-Driven Reaction Analysis for Pharmaceutical Process Development. *Ind Eng Chem Res* **2020**, *59* (6), 2409–2421. <https://doi.org/10.1021/acs.iecr.9b03578>.
- (4) Farina, V. How to Develop Organometallic Catalytic Reactions in the Pharmaceutical Industry. *Organic Process Research and Development*. American Chemical Society May 19, 2023, pp 831–846. <https://doi.org/10.1021/acs.oprd.3c00086>.
- (5) Wei, B.; Sharland, J. C.; Lin, P.; Wilkerson-Hill, S. M.; Fullilove, F. A.; McKinnon, S.; Blackmond, D. G.; Davies, H. M. L. In Situ Kinetic Studies of Rh(II)-Catalyzed Asymmetric Cyclopropanation with Low Catalyst Loadings. *ACS Catal* **2020**, *10* (2), 1161–1170. <https://doi.org/10.1021/acscatal.9b04595>.

- (6) Baxter, R. D.; Sale, D.; Engle, K. M.; Yu, J. Q.; Blackmond, D. G. Mechanistic Rationalization of Unusual Kinetics in Pd-Catalyzed C-H Olefination. *J Am Chem Soc* **2012**, *134* (10), 4600–4606. <https://doi.org/10.1021/ja207634t>.
- (7) Braddock, D. C.; Rowley, B. C.; Lickiss, P. D.; Fussell, S. J.; Qamar, R.; Pugh, D.; Rzepa, H. S.; White, A. J. P. On the Use of Triarylsilanols as Catalysts for Direct Amidation of Carboxylic Acids. *Journal of Organic Chemistry* **2023**, *88* (14), 9853–9869. <https://doi.org/10.1021/acs.joc.3c00585>.
- (8) Higham, J. I.; Bull, J. A. Amine-Catalyzed Copper-Mediated CH Sulfonylation of Benzaldehydes via a Transient Imine Directing Group. **2022**. <https://doi.org/10.26434/chemrxiv-2021-bhs2k-v2>.
- (9) Newton, O. J.; Hellgardt, K.; Richardson, J.; Hii, K. K. M. ‘Homeopathic’ Palladium Catalysis? The Observation of Distinct Kinetic Regimes in a Ligandless Heck Reaction at (Ultra-)Low Catalyst Loadings. *J Catal* **2023**, *424*, 29–38. <https://doi.org/10.1016/j.jcat.2023.05.005>.
- (10) Servia, M. Á. de C.; Sandoval, I. O.; Hellgardt, K.; Kuok, K.; Hii, Zhang, D.; Chanona, E. A. del R. The Automated Discovery of Kinetic Rate Models -- Methodological Frameworks. *ArXiv* **2023**.
- (11) Hessel, V.; Kralisch, D.; Kockmann, N.; Noël, T.; Wang, Q. Novel Process Windows for Enabling, Accelerating, and Uplifting Flow Chemistry. *ChemSusChem* **2013**, *6* (5), 746–789. <https://doi.org/10.1002/cssc.201200766>.
- (12) Cox, B. G. Complex Reactions. In *Modern Liquid Phase Kinetics*; Oxford university press: Oxford, 1994; p 27.
- (13) Brigham, E. C.; Meyer, G. J. Ostwald Isolation to Determine the Reaction Order for $\text{TiO}_2(\text{e}^-)|\text{S}+\leftrightarrow\text{TiO}_2|\text{S}$ Charge Recombination at Sensitized TiO_2 Interfaces. *Journal of Physical Chemistry C* **2014**, *118* (15), 7886–7893. <https://doi.org/10.1021/jp501814r>.
- (14) Zhang, S.; Zhang, J.; Zou, H. C(Sp³)-H Oxygenation via Alkoxy-palladium(II) Species: An Update for the Mechanism. *Chem Sci* **2022**, *13* (5), 1298–1306. <https://doi.org/10.1039/d1sc06907a>.
- (15) Espenson, J. H.; Pestovsky, O.; Huston, P.; Staudt, S. *Organometallic Catalysis in Aqueous Solution: Oxygen Transfer to Bromide*; 1994; Vol. 116.
- (16) Deem, M. C.; Cai, I.; Derasp, J. S.; Prieto, P. L.; Sato, Y.; Liu, J.; Kukor, A. J.; Hein, J. E. Best Practices for the Collection of Robust Time Course Reaction Profiles for Kinetic Studies. *ACS Catalysis*. American Chemical Society January 20, 2023, pp 1418–1430. <https://doi.org/10.1021/acscatal.2c05045>.
- (17) Blackmond, D. G. Reaction Progress Kinetic Analysis: A Powerful Methodology for Mechanistic Studies of Complex Catalytic Reactions.

- Angewandte Chemie - International Edition* **2005**, *44* (28), 4302–4320.
<https://doi.org/10.1002/anie.200462544>.
- (18) Burés, J. A Simple Graphical Method to Determine the Order in Catalyst. *Angewandte Chemie* **2016**, *128* (6), 2068–2071.
<https://doi.org/10.1002/ange.201508983>.
- (19) Burés, J. Variable Time Normalization Analysis: General Graphical Elucidation of Reaction Orders from Concentration Profiles. *Angewandte Chemie - International Edition* **2016**, *55* (52), 16084–16087.
<https://doi.org/10.1002/anie.201609757>.
- (20) Cano, I.; Weilhard, A.; Martin, C.; Pinto, J.; Lodge, R. W.; Santos, A. R.; Rance, G. A.; Åhlgren, E. H.; Jónsson, E.; Yuan, J.; Li, Z. Y.; Licence, P.; Khlobystov, A. N.; Alves Fernandes, J. Blurring the Boundary between Homogenous and Heterogeneous Catalysis Using Palladium Nanoclusters with Dynamic Surfaces. *Nat Commun* **2021**, *12* (1), 2–7.
<https://doi.org/10.1038/s41467-021-25263-6>.
- (21) Durin, G.; Fontaine, A.; Berthet, J.; Nicolas, E.; Thuéry, P.; Cantat, T. Metal-Free Catalytic Hydrogenolysis of Silyl Triflates and Halides into Hydrosilanes**. *Angewandte Chemie* **2022**, *134* (23), 1–5.
<https://doi.org/10.1002/ange.202200911>.
- (22) Liu, W.; Lavagnino, M. N.; Gould, C. A.; Macmillan, D. W. C. A Biomimetic SH₂ Cross-Coupling Mechanism for Quaternary Sp³-Carbon Formation. **2021**, *2* (December), 1258–1263.
- (23) Sean, C. *Kinalite Example*. GitLab.
https://gitlab.com/heingroup/kinalite_example/-/blob/master/main.py.
accessed 22.03.2024.
- (24) Sean, C. *kinalite 0.0.6*. The Python Package Index.
<https://pypi.org/project/kinalite/>. accessed 22.03.2024.
- (25) Bork, F.; Clark, S.; Burland, P.; Sale, D.; Hein, J. Kinalite A User-Friendly Online Tool for Automated Variable Time Normalization Analysis (VTNA). *Pre-print* **2024**. <https://doi.org/10.26434/chemrxiv-2024-m15pr>.
- (26) Nielsen, C. D. T.; Burés, J. Visual Kinetic Analysis. *Chem Sci* **2019**, *10* (2), 348–353. <https://doi.org/10.1039/c8sc04698k>.
- (27) Xia, J.; Hirai, T.; Katayama, S.; Nagae, H.; Zhang, W.; Mashima, K. Mechanistic Study of Ni and Cu Dual Catalyst for Asymmetric C-C Bond Formation; Asymmetric Coupling of 1,3-Dienes with C-Nucleophiles to Construct Vicinal Stereocenters. *ACS Catal* **2021**, *11*, 6643–6655.
<https://doi.org/10.1021/acscatal.1c01626>.
- (28) Burés, J. Variable Time Normalization Analysis: General Graphical Elucidation of Reaction Orders from Concentration Profiles. *Angewandte Chemie - International Edition* **2016**, *55* (52), 16084–16087.
<https://doi.org/10.1002/anie.201609757>.

- (29) Murray, K.; Müller, S.; Turlach, B. A. Revisiting Fitting Monotone Polynomials to Data. *Comput Stat* **2013**, *28* (5), 1989–2005. <https://doi.org/10.1007/s00180-012-0390-5>.
- (30) Bon, J. J.; Murray, K.; Turlach, B. A. Fitting Monotone Polynomials in Mixed Effects Models. *Stat Comput* **2019**, *29* (1), 79–98. <https://doi.org/10.1007/s11222-017-9797-8>.
- (31) Pabst, T. P.; Obligacion, J. V.; Rochette, É.; Pappas, I.; Chirik, P. J. Cobalt-Catalyzed Borylation of Fluorinated Arenes: Thermodynamic Control of C(Sp²)-H Oxidative Addition Results in Ortho-to-Fluorine Selectivity. *J Am Chem Soc* **2019**, *141* (38), 15378–15389. <https://doi.org/10.1021/jacs.9b07984>.
- (32) Davis-Gilbert, Z. W.; Wen, X.; Goodpaster, J. D.; Tonks, I. A. Mechanism of Ti-Catalyzed Oxidative Nitrene Transfer in [2 + 2 + 1] Pyrrole Synthesis from Alkynes and Azobenzene. *J Am Chem Soc* **2018**, *140* (23), 7267–7281. <https://doi.org/10.1021/jacs.8b03546>.
- (33) Tran, G.; Shao, W.; Mazet, C. Ni-Catalyzed Enantioselective Intermolecular Hydroamination of Branched 1,3-Dienes Using Primary Aliphatic Amines. *J Am Chem Soc* **2019**, *141* (37), 14814–14822. <https://doi.org/10.1021/jacs.9b07253>.
- (34) Antermite, D.; White, A. J. P.; Casarrubios, L.; Bull, J. A. On the Mechanism and Selectivity of Palladium-Catalyzed C(Sp³)-H Arylation of Pyrrolidines and Piperidines at Unactivated C₄ Positions: Discovery of an Improved Dimethylaminoquinoline Amide Directing Group. *ACS Catal* **2023**, *13* (14), 9597–9615. <https://doi.org/10.1021/acscatal.3c01980>.
- (35) Day, D. M.; Farmer, T. J.; Sherwood, J.; Clark, J. H. An Experimental Investigation into the Kinetics and Mechanism of the Aza-Michael Additions of Dimethyl Itaconate. *Tetrahedron* **2022**, *121*, 132921. <https://doi.org/10.1016/j.tet.2022.132921>.
- (36) Day, D. M.; Farmer, T. J.; Granelli, J.; Lofthouse, J. H.; Lynch, J.; McElroy, C. R.; Sherwood, J.; Shimizu, S.; Clark, J. H. Reaction Optimization for Greener Chemistry with a Comprehensive Spreadsheet Tool. *Molecules* **2022**, *27* (23), 1–12. <https://doi.org/10.3390/molecules27238427>.
- (37) Matviitsuk, A.; Greenhalgh, M. D.; Antúnez, D. B.; Slawin, A. M. Z.; Smith, A. D. Aryloxide-Facilitated Catalyst Turnover in Enantioselective α , β -Unsaturated Acyl Ammonium Catalysis. *Angewandte Chemie* **2017**, *129* (40), 12450–12455. <https://doi.org/10.1002/ange.201706402>.
- (38) Margarita, C.; Villo, P.; Tuñón, H.; Dalla-Santa, O.; Camaj, D.; Carlsson, R.; Lill, M.; Ramström, A.; Lundberg, H. Zirconium-Catalysed Direct Substitution of Alcohols: Enhancing the Selectivity by Kinetic Analysis. *Catal Sci Technol* **2021**, *11* (22), 7420–7430. <https://doi.org/10.1039/d1cy01219c>.

- (39) Davis-Gilbert, Z. W.; Wen, X.; Goodpaster, J. D.; Tonks, I. A. Mechanism of Ti-Catalyzed Oxidative Nitrene Transfer in [2 + 2 + 1] Pyrrole Synthesis from Alkynes and Azobenzene. *J Am Chem Soc* **2018**, *140* (23), 7267–7281. <https://doi.org/10.1021/jacs.8b03546>.
- (40) Nishii, Y.; Ikeda, M.; Hayashi, Y.; Kawauchi, S.; Miura, M. TriptycenyI Sulfide: A Practical and Active Catalyst for Electrophilic Aromatic Halogenation Using N-Halosuccinimides. *J Am Chem Soc* **2020**, *142* (3), 1621–1629. <https://doi.org/10.1021/jacs.9b12672>.
- (41) Pfeffer, C.; Wannemacher, N.; Frey, W.; Peters, R. Stereo- A Nd Regioselective Dimerization of Alkynes to Enynes by Bimetallic Syn-Carbopalladation. *ACS Catal* **2021**, *11* (9), 5496–5505. <https://doi.org/10.1021/acscatal.1c00473>.
- (42) Smith, S. M.; Greenhalgh, M. D.; Feoktistova, T.; Walden, D. M.; Taylor, J. E.; Cordes, D. B.; Slawin, A. M. Z.; Cheong, P. H. Y.; Smith, A. D. Scope, Limitations and Mechanistic Analysis of the HyperBTM-Catalyzed Acylative Kinetic Resolution of Tertiary Heterocyclic Alcohols**. *European J Org Chem* **2022**, *2022* (1). <https://doi.org/10.1002/ejoc.202101111>.
- (43) Braddock, D. C.; Lancaster, B. M. J.; Tighe, C. J.; White, A. J. P. Surmounting Byproduct Inhibition in an Intermolecular Catalytic Asymmetric Alkene Bromoesterification Reaction as Revealed by Kinetic Profiling. *Journal of Organic Chemistry* **2023**, *88* (13), 8904–8914. <https://doi.org/10.1021/acs.joc.3c00672>.
- (44) Herbort, J. H.; Lalissee, R. F.; Hadad, C. M.; Rajanbabu, T. V. Cationic Co(I) Catalysts for Regiodivergent Hydroalkenylation of 1,6-Enynes: An Uncommon Cis-β-C-H Activation Leads to Z-Selective Coupling of Acrylates. *ACS Catal* **2021**, *11* (15), 9605–9617. <https://doi.org/10.1021/acscatal.1c02530>.
- (45) Antico, E.; Leutzsch, M.; Wessel, N.; Weyhermüller, T.; Werlé, C.; Leitner, W. Selective Oxidation of Silanes into Silanols with Water Using [MnBr(CO)₅] as a Precatalyst. *Chem Sci* **2022**, *14* (1), 54–60. <https://doi.org/10.1039/d2sc05959b>.
- (46) McLaughlin, C.; Slawin, A. M. Z.; Smith, A. D. Base-free Enantioselective C(1)-Ammonium Enolate Catalysis Exploiting Aryloxides: A Synthetic and Mechanistic Study. *Angewandte Chemie* **2019**, *131* (42), 15255–15263. <https://doi.org/10.1002/ange.201908627>.
- (47) Aikonen, S.; Muuronen, M.; Wirtanen, T.; Heikkinen, S.; Musgreave, J.; Burés, J.; Helaja, J. Gold(I)-Catalyzed 1,3-O-Transposition of Ynones: Mechanism and Catalytic Acceleration with Electron-Rich Aldehydes. *ACS Catal* **2018**, *8* (2), 960–967. <https://doi.org/10.1021/acscatal.7b04262>.

- (48) McLaughlin, C.; Smith, A. D. Enantioselective Isothiourea Catalysis via C(1)-Ammonium Enolate Intermediates : Applications and Mechanistic Studies, University of St. Andrews, St. Andrews, 2021.
- (49) Elsby, M. R.; Son, M.; Oh, C.; Martin, J.; Baik, M. H.; Baker, R. T. Mechanistic Study of Metal-Ligand Cooperativity in Mn(II)-Catalyzed Hydroborations: Hemilabile SNS Ligand Enables Metal Hydride-Free Reaction Pathway. *ACS Catal* **2021**, *11* (15), 9043–9051. <https://doi.org/10.1021/acscatal.1c02238>.
- (50) Tran, G.; Shao, W.; Mazet, C. Ni-Catalyzed Enantioselective Intermolecular Hydroamination of Branched 1,3-Dienes Using Primary Aliphatic Amines. *J Am Chem Soc* **2019**, *141* (37), 14814–14822. <https://doi.org/10.1021/jacs.9b07253>.